Vol. 81: 1–14, 2020
https://doi.org/10.3354/cr01606

CLIMATE RESEARCH
Clim Res

Published online July 2

Reconstruction of maximum temperature on Zhegu Mountain, western Sichuan Plateau (China)

Maierdang Keyimu[1], Zongshan Li[1,*], Yijin Zhao[1], Yanjun Dong[1], Bojie Fu[1], Zexin Fan[2], Xiaochun Wang[3]

[1]State Key Laboratory of Urban and Regional Ecology, Research Center for Eco-Environmental Science, Chinese Academy of Sciences, Beijing 100085, PR China
[2]Xishuangbanna Tropical Botanical Garden, Chinese Academy of Sciences, Mengla 666303, PR China
[3]College of Forestry, Northeast Forestry University, Harbin 150040, PR China

ABSTRACT: Historical temperature reconstructions at high altitudes are still insufficient in southwestern China, which is considered one of the most sensitive areas to climate change in the world. Here we developed a tree ring-width chronology of Faxon fir *Abies fargesii* var. *faxoniana* at the upper timber line on Zhegu Mountain, Miyaluo Scenic Area, western Sichuan, China. The climate–tree growth relationship analysis indicated temperature as the dominant regulator on radial tree growth in this region. The reconstruction of aggregated maximum temperature (TMX) of autumn and winter for the period 1856–2016 was achieved with a linear regression model that accounted for 43.6% of the actual variability in the common time series (1954–2016). The reconstruction identified 4 warm periods and 3 cold periods. Similarities of warm and cold periods with previously published reconstructions from nearby sites indicated the reliability of our reconstruction. The significant positive correlation between TMX reconstruction and the Asian-Pacific Oscillation index and the Atlantic Multi-decadal Oscillation index suggested a linkage between large-scale climate circulations and the thermal variability at a multi-decadal scale on the western Sichuan Plateau. We also found that solar activity exerted a strong influence on decadal temperature variability in this region. The cold periods were matched well with historical large volcanic eruptions. Our results strengthen the historical climatic information in southwestern China and contribute to further understanding the regional thermal variability as well as its driving mechanism.

KEY WORDS: Tree ring · Aggregated maximum temperature · Climate reconstruction · Western Sichuan Plateau

1. INTRODUCTION

To better predict future climate change, we must understand the features of present and past climate, but it is difficult to track the course of climate history due to lack of instrumental climate records before the 1950s (Esper et al. 2012). Therefore, we have to rely on other proxies, including ice cores (Steiger et al. 2017), speleothems (Proctor et al. 2000, Vaks et al. 2003), pollen (Jiménez-Moreno et al. 2010), lake sediments (Zech et al. 2009), and tree rings (Fritts 1976, Pilcher et al. 1984, Schweingruber 1996, Yang et al. 2014), to obtain historical climate information and reveal features of variability. Tree rings are frequently used proxies in paleoclimatic studies (Esper et al. 2002, Zhang et al. 2003,

*Corresponding author: zsli_st@rcees.ac.cn

Björklund et al. 2019). In dendroclimatology, tree-ring variables are used to examine radial tree growth–climate relationships and accordingly reconstruct historical climate records (Briffa et al. 1996, Allen et al. 2019). Tree-ring width is primarily used due to its simplicity of measurement and crossdating (Fritts 1976, D'Arrigo et al. 2008, Gou et al. 2015, Huang et al. 2019).

The accelerated temperature increase globally since the late 20th century is undeniable (IPCC 2013), and although increases of minimum temperatures are more prominent, we should also pay attention to variability in maximum temperature (Wilson & Luckman 2002). Maximum temperature is an important factor in forest growth as an upper boundary of temperature for photosynthetic activity and carbon assimilation. Reconstruction of maximum temperature could therefore contribute to forest ecosystem prediction models.

The western Sichuan Plateau is located between the Tibetan Plateau and Sichuan Basin of China. According to the IPCC (2013), it is one of the most sensitive areas to climate change. Subalpine coniferous forests dominate this area and play an important role in water and soil conservation in the head stream region of the Yangtze River (Pang et al. 2009). There are many tree line ecotones in the western Sichuan Plateau, and most of the upper tree lines comprise Faxon fir *Abies fargesii* var. *faxoniana*. Unfortunately, few dendroclimatological investigations have been made on the topic of historical temperature reconstruction in this area (Shao & Fan 1999, Song et al. 2007, Li et al. 2015, Zhu et al. 2016), and even fewer in the case of fir trees (Li et al. 2010, Zhu et al. 2016). Furthermore, the linkage between the regional historical temperature variability and large-scale atmospheric circulation as well as possible forcing mechanisms have received scant attention.

In the present investigation, we analyzed growth–climate response using a tree-ring width series of Faxon fir from the timberline of Zhegu Mountain in the Miyaluo Scenic Area, western Sichuan Plateau, and present an aggregated autumn and winter maximum temperature reconstruction for this area spanning the period 1856–2016. The reconstructed series helps to further understand the climate variation history in western Sichuan during the past 16 decades and the connection of regional temperature fluctuation with global-scale climate circulations as well as driving mechanisms. The aims of our investigation were to (1) establish a tree-ring width chronology of Faxon fir at the upper treeline in the western Sichuan Plateau, (2) examine the growth–climate relationships and reconstruct the aggregated autumn and winter maximum temperature, (3) investigate the representativeness of the reconstructed series over a large-scale geographic extent, and (4) analyze the features of temperature variability and its connection with climate forcing.

2. MATERIALS AND METHODS

2.1. Study area and sampling site

The study area is situated on Zhegu Mountain in the Miyaluo Scenic Area (31.65° N, 102.78° E) in the western Sichuan Plateau of China, which is a part of the Hengduan Mountains (Fig. 1). The climate of this area is influenced by the air masses from the Pacific and Indian Oceans as well as the Tibetan Plateau. The Indian Ocean monsoon from the southwest and the Pacific Ocean monsoon from the southeast bring precipitation to this region during the summer. The winter is cold and dry and is affected by a cold airstream which comes from the Tibetan Plateau. The nearest China Meteorological Administration weather station in this region is located in Maerkang at 2664 m a.s.l. The linear distance from the weather station to the tree-ring sampling site is approximately 60 km. According to the climate data, the annual mean temperature is 6–12°C, and the mean temperatures in January and July are –8°C and 12.6°C, respectively. The range of annual mean precipitation is 600–1100 mm. The recent climate showed obvious rising temperature and relatively stable variation in precipitation (Fig. 2). The topography of the sampling site is steep, and it is not favorable for the development of soil; thus, only a thin layer of alpine meadow soil covers the bedrock. The forests in this region consist of various subalpine evergreen tree species, including *A. faxoniana*, *A. ernestii*, *Picea asperata*, *P. purpurea*, *P. wilsonii*, *Tsuga chinensis*, *Rhododendron simsii*, *Pinus armandii*, and *Quercus aquifolioides*, distributed at different altitudes on Zhegu Mountain. We collected tree ring samples at 4150 m a.s.l., which is the upper tree line in this region. We selected trees without signs of injury, then extracted tree ring samples at breast height (1.3 m) using a 5 mm diameter Swedish increment borer. To avoid the possible influence of tension wood on radial tree growth, we sampled along an axis perpendicular to the slope inclination. Altogether, 40 tree-ring cores were sampled from 20 trees.

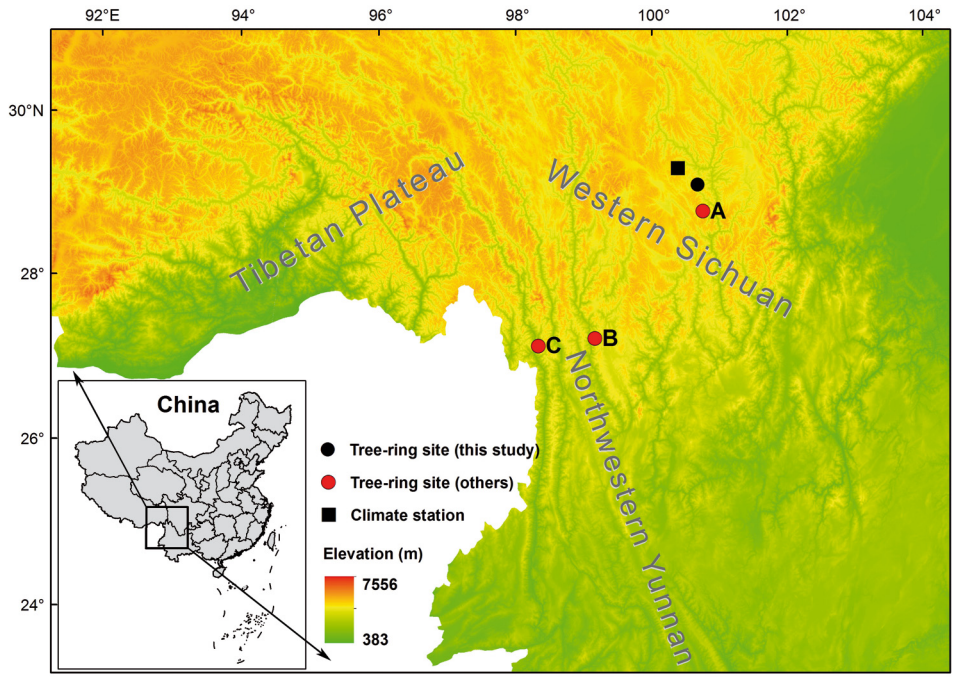

Fig. 1. Tree-ring sampling site and climate station on Zhegu Mountain in the Miyaluo Scenic Area, western Sichuan Plateau, China. Previously investigated sites are located in A: Miyaluo Forest Reserve Zone (Li et al. 2015); B: Big Snow Mountain (Keyimu et al. 2020b); and C: Hengduan Mountains (Fan et al. 2009)

2.2. Establishment of tree-ring chronology

The tree-ring samples were treated following standard procedures of dendrochronology experiments (Stokes & Smiley 1996). In the laboratory, tree-ring cores were mounted after air-drying and sanded progressively with 400-, 800-, and 1200-grit sandpaper, then scanned using a TSD4800 flatbed scanner to generate a digital image for dendrochronological analysis. We used the WinDENDRO ver. 2017a tree-ring measurement system to obtain the ring width (details of methods are available in Keyimu et al. 2020a); the accuracy of measurement was 0.001. Crossdating was done visually by marking tree-ring samples with a pencil under the microscope, and then crossdating quality was checked using COFECHA software (Holmes 1983). We ultimately used 29 tree-ring samples from 15 trees. We used the nega-

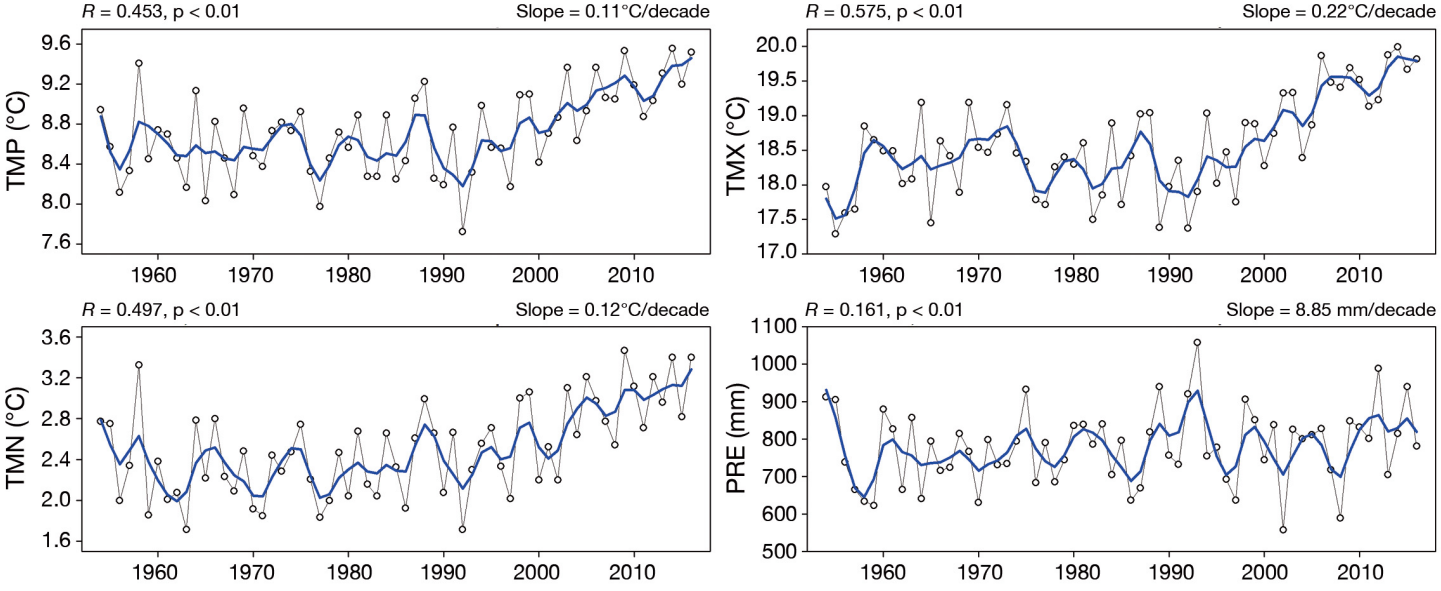

Fig. 2. Climate-change trends recorded by a meteorological station near the tree-ring sampling site on Zhegu Mountain. TMP: annual mean temperature; TMN: annual minimum temperature; TMX: annual maximum temperature; PRE: annual total precipitation. The blue thick line in each sub-plot is the 5 yr loess-smoothed series

tive exponential model method to eliminate the age dependency of radial tree growth (Cook et al. 1995, Zhang et al. 2003), and then established the standard chronology of tree-ring width following the method of Keyimu et al. (2020a). Detrending and chronology establishment were processed using the 'dplR' dendrochronology package within R (version 3.5.1) statistical software (R Core Team 2019).

2.3. Climate data

We used climate data from the Maerkang meteorological station near our tree-ring sampling site for calibrating the tree-ring data. Climate variables include monthly maximum (TMX), minimum (TMN), and mean (TMP) temperatures, and monthly total precipitation (PRE). The length of the climate record was 63 yr (1954–2016).

2.4. Data analysis

The relationships between climate and tree growth were determined by conducting Pearson correlation analysis for the period 1954–2016. Considering the legacy effect of previous-year climate factors on radial tree growth in the current year, we calculated correlations covering 18 months (previous June to current November). The climate growth correlations were calculated using the 'treeclim' package in R, and the 95% confidence interval was used to evaluate the correlation. We employed a linear regression model for the reconstruction. The leave-one-out cross verification method was used to evaluate the fidelity of the reconstruction model (Yin et al. 2015). In addition, Pearson's correlation coefficient (r), explained variance (R^2), adjusted explained variance (R_{adj}^2), reduction of error (RE), sign test (ST), coefficient of efficiency (CE), product mean test (PMT), and Durbin-Watson test (DW) were used to evaluate the results of the reconstruction.

3. RESULTS

3.1. Chronology statistics

The statistics of tree-ring width chronology are shown in Table 1. The length of the chronology was 161 yr (1856–2016) (Fig. 3) including a minimum of 5 tree-ring samples. The mean correlation among tree-ring series (Rbar) was 0.47, and the variance in the first eigenvector was 29.41%, implying a strong common signal among the individual trees in the chronology. Our chronology was therefore considered suitable for studying the climate history of Zhegu Mountain. The mean sensitivity was 0.19. The signal to noise ratio was 5.57. Standard deviation (SD), i.e. the variability in the chronology due to outside influences, was 0.43. The average value of the expressed population signal (EPS) was 0.90. According to the EPS value, the chronology was robust until 1869, but overall descriptive statics indicated that our chronology contained relatively strong climatic information. A first-order autocorrelation value of 0.57 implied a strong influence of previous-year growth conditions on the current-year tree growth.

3.2. Climate–growth response

The results of the correlation analysis between climate variables and tree-ring width chronology showed that the radial tree growth–temperature correlations were all positive during the analyzed time window except in current May for TMP (R = −0.08) and TMN (R = −0.07), and previous August for TMX (R = −0.08). Compared to temperature, PRE exerted less impact on tree growth. Based on the results of correlation analysis, we confirmed that temperature was the dominant factor in the radial growth of *Abies fargessi var. faxoniana* on Zhegu Mountain (Fig. 4). The correlation coefficient of tree-ring width chronology with TMX was higher than those with TMP and TMN. The correlation between aggregated

Table 1. Summary statistics for tree-ring width chronologies of *Abies fargessi var. faxoniana* on Zhegu Mountain, western Sichuan Plateau, China. MS: mean sensitivity, AR1: first-order autocorrelation, Rbar: mean inter-series correlation, SNR: signal-to-noise ratio, EPS: expressed population signal, VFE: variance in first eigenvector

Type	Location	Time period	Elevation (m)	Cores (n)	SD	MS	AR1	Rbar[a]	SNR[a]	EPS[a]	VFE (%)[a]
Tree-ring site	31.65° N, 102.78° E	1856–2017	4150	29	0.43	0.19	0.57	0.42	5.57	0.90	29.41
Climate station	31.9° N, 102.23° E	1954–2016	2664	–	–	–	–	–	–	–	–

[a]Calculation for the common intervals of the chronologies

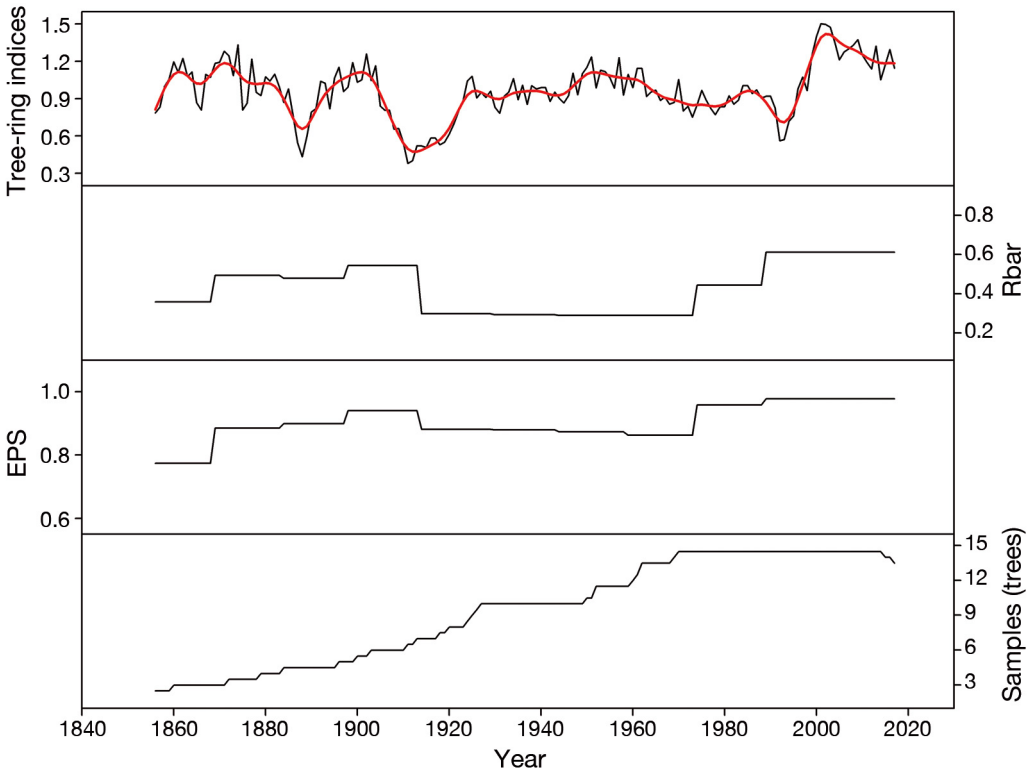

Fig. 3. Tree-ring standard chronology (black thin line is the raw data series, and red thick line is the 11 yr loess-smoothed series), mean inter-series correlation (Rbar), the expressed population signal (EPS), and the sample size. Rbar and EPS were calculated using a 30 yr window that lags 15 yr

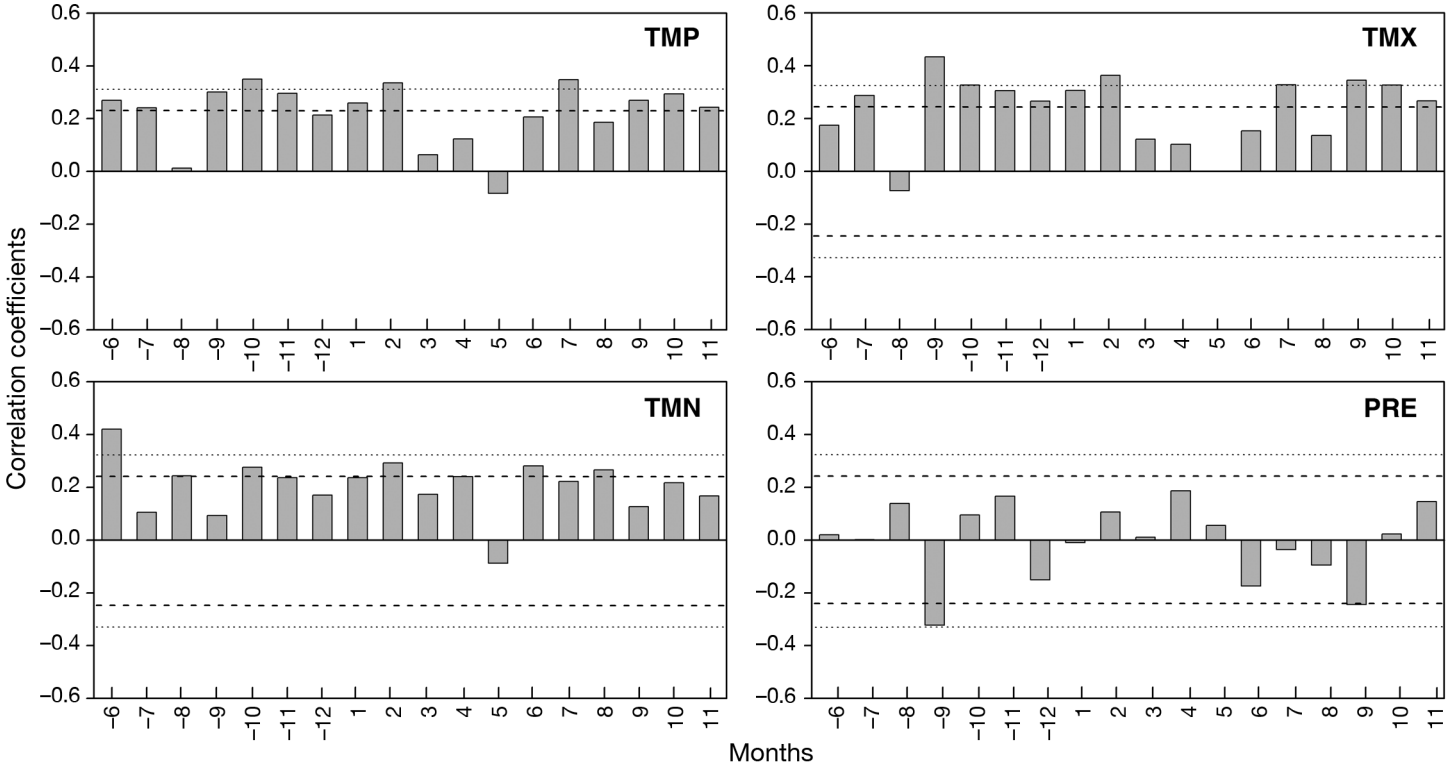

Fig. 4. Correlation results between tree-ring indices and climate data for Zhegu Mountain. Climate data are from the meteorological station, including monthly mean temperature (TMP), minimum temperature (TMN), maximum temperature (TMX), and precipitation (PRE). Correlations were calculated from June of the previous year ('−6' on the *x*-axis) to November of the current year ('11') over the common period (1954–2016). Horizontal dashed and dotted lines denote the 95 and 99% significance levels

TMX of autumn and winter (September–February) and tree-ring width chronology was higher (R = 0.66, p < 0.01) (Fig. 5). The moving correlation analysis showed that the correlation coefficients between tree-ring indices and aggregated TMX were higher than the confidence interval of 95% during most of the investigation period (Fig. 6), indicating that the relationship was in compliance with the uniformitarian principle of tree-ring-based climate reconstruction. Therefore, we chose to reconstruct the aggregated TMX of autumn and winter.

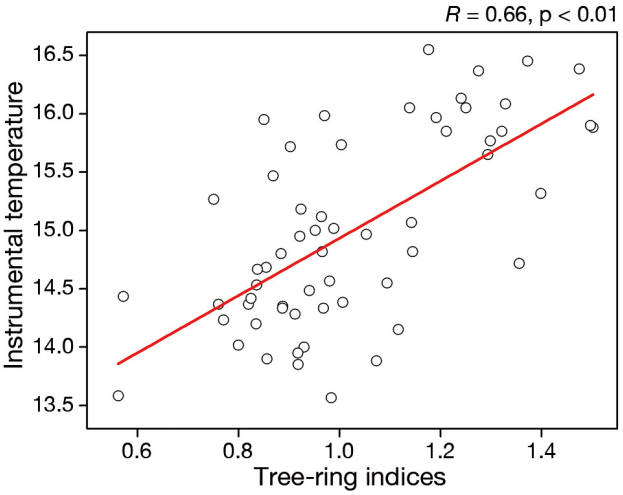

Fig. 5. Tree-ring indices of *Abies fargessi var. faxoniana* and aggregated maximum temperature of autumn and winter during the period of 1954–2016

3.3. Temperature reconstruction

Based on the relationship between TMX and the chronology, we developed a linear regression model (y = 0.2454x + 12.48) and reconstructed the aggregated TMX of autumn and winter for Zhegu Mountain that extended back to 1856 (Fig. 7b). The results showed that the reconstruction accounted for 43.2% (R_{adj}^2 = 42.2%) of the actual temperature variance in the time series of 1954–2016, and the developed model passed all conventional verification tests (Table 2). Fig. 7a shows that our aggregated TMX reconstruction series was parallel with the overall variation of instrumental data dur-

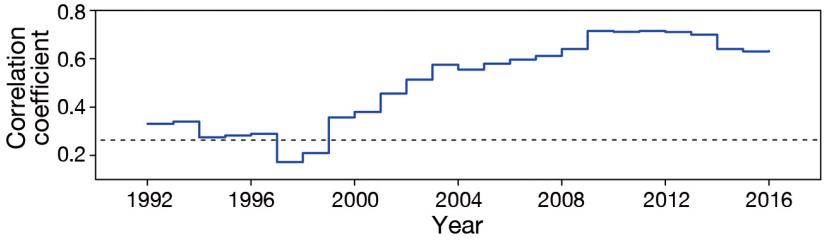

Fig. 6. Moving correlation analysis between the tree-ring width chronology and the aggregated maximum temperature in autumn and winter. The horizontal dashed line represents the 95% significance level of the correlation

Fig. 7. (a) Instrumental and reconstructed temperature during the common period 1954–2016. (b) Reconstructed maximum temperature (TMX) of aggregated autumn and winter on Zhegu Mountain, plotted annually from 1856–2016 (black thin line), along with an 11 yr loess smoothing (thick red line). The horizontal black line represents the average of reconstructed TMX series, and the dashed lines represent the standard deviation from the mean value. A–F represent years in which volcanic eruptions occurred (see Table 3)

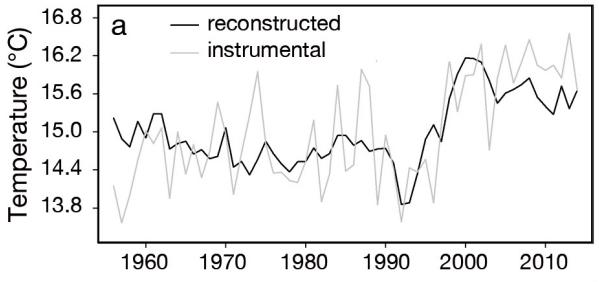

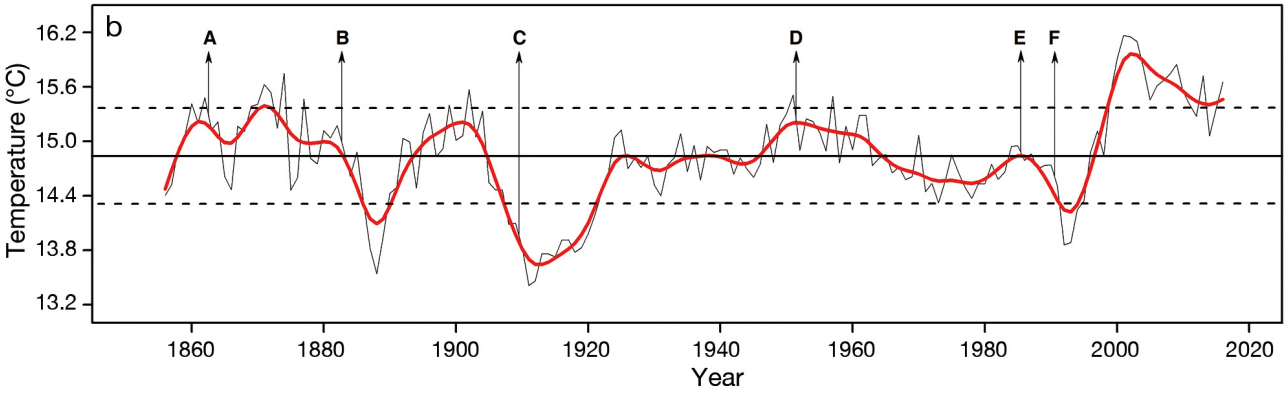

Table 2. Statistics of leave-one-out verification for tree-ring reconstruction of annual temperature in the period 1954–2016 for Zhegu Mountain. Sign-test: sign of paired observed and estimated departures from their mean on the basis of the number of agreements/disagreements; PMT: product mean test; RE: reduction of error; CE: coefficient of efficiency; DW Durbin–Watson test; $^{*}p < 0.05$, $^{**}p < 0.01$

	R	R^2	R_{adj}^2	*F*	Sign-test	PMT	RE	CE	DW
Calibration	0.657	0.436	0.422	–	–	–	–	–	–
Verification	0.615	0.378	0.358	37.65**	52+/12–*	11.95*	0.31	0.25	1.67

ing the correlation period. The positive values of RE and CE (0.31 and 0.25, respectively) support the legitimacy of our reconstruction. In addition, the results of the ST and PMT indicated the validity of reconstruction by detecting the difference between measured climatic data and estimations from the leave-one-out method. Results of statistical tests confirmed the robustness of the regression model, and we used it to reconstruct the aggregated TMX of autumn and winter for the past 161 yr.

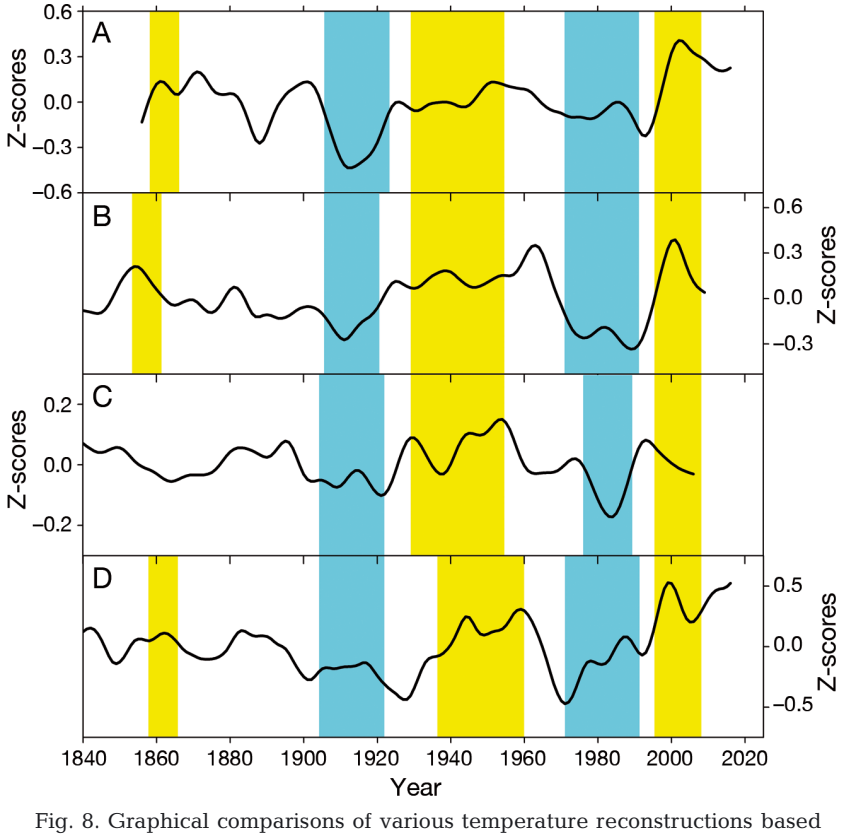

Fig. 8. Graphical comparisons of various temperature reconstructions based on tree-ring records in southwestern China in different studies. (a) Aggregated autumn and winter maximum temperature reconstruction in the present study. (b) Annual mean temperature reconstruction in the western Sichuan Province of China (Li et al. 2015). (c) Warm season (April–September) mean temperature reconstruction in the central Hengduan Mountains (Fan et al. 2009). (d) Annual mean minimum temperature reconstruction in the southeastern edge of the Tibetan Plateau (Keyimu et al. 2020b). All reconstructions were *Z*-scored and 11 yr loess smoothed. Yellow and cyan bars show the warm and cold periods, respectively

3.4. Characteristics of TMX reconstruction

Fig. 7b depicts the aggregated autumn and winter TMX series reconstructed for the last 161 yr (1856–2016). The mean of the reconstructed TMX was 14.84°C, and the standard deviation was 0.54°C. We pre-defined the years which exceeded mean TMX as warm years, while those below were considered cold years. Years exceeding 15.38°C were extreme warm years, while years below 14.3°C were extreme cold years. Our reconstruction showed alternating periods of cool and warm records, but the periods were different in length and amplitude. According to the reconstruction, the warm periods were 1860s–1880s, 1895–1905, 1950s–1965, and 1995 until present; In contrast, marked periods with low temperatures occurred during 1885–1890s, 1905–1925, 1965–1995. Moreover, 1887–1889, 1908–1921, and 1992–1993 were extremely cold years, while 1871–1872, 1874, 1902, 1951, 1957, and 1999–2010 were extremely warm years. Some of the warm and cold periods were synchronized with other reconstructions from the surrounding regions (Fig. 8). In addition, according to Fig. 9, the reconstructed TMX series was able to represent climate conditions over a large area in the western Sichuan region. From the reconstruction series, we can confirm that the extreme warm years that have occurred since 2000 are unprecedented in the study area. Fig. 10 shows the correlation between TMX reconstruction in present study with global sea surface temperature (HadISST1 1°), which indicates the spatial linkage of the reconstructed TMX series on Zhegu Mountain with a global climate system. Fig. 7b shows that a significant decline in temperature occurred in the year following major volcanic events

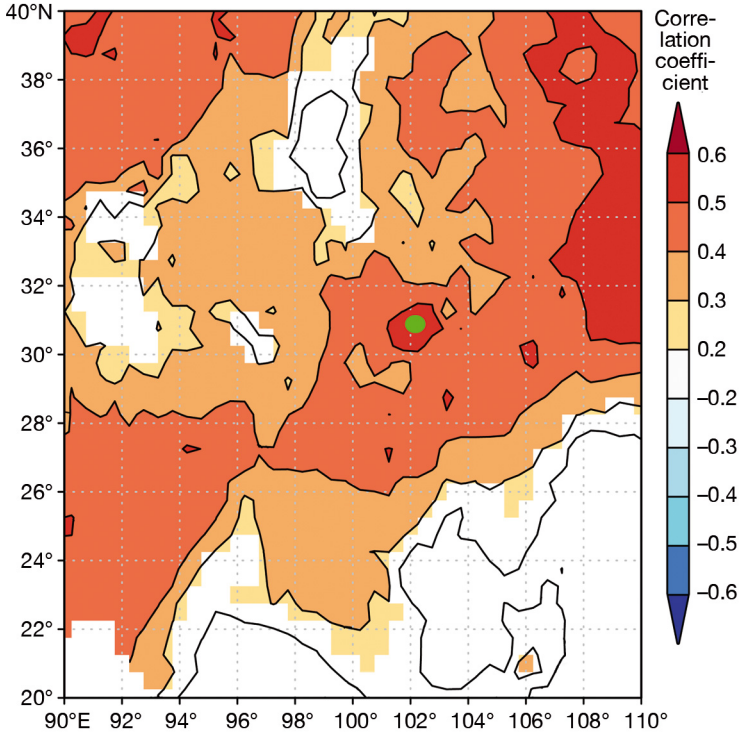

Fig. 9. Spatial correlations of the reconstructed maximum temperature of aggregated seasons of autumn and winter and the regional gridded maximum temperature from the CRU TS 4.03 dataset for 1954 2016. The analyses were performed using the KNMI climate explorer (Royal Netherlands Meteorological Institute; http://climexp.knmi.nl). The gridded climate dataset was developed by the Climatic Research Unit (Mitchell & Jones 2005; CRU TS4.03). The green circle represents the study area

(detailed in Table 3), and this was supported by the results of the superposed epoch analysis.

4. DISCUSSION

4.1. Tree growth and climate relationships

The climate–tree growth response analysis confirmed that temperature was the main regulator of radial growth in Faxon fir on Zhegu Mountain in the western Sichuan Plateau of China. *Abies* spp. grow at higher elevations compared to other coniferous species in this region (Zhang 2006). Dendroclimatological investigations at high elevations, especially near the tree line, have suggested that temperature mainly controls tree growth (Li et al. 2011, Zhu et al. 2016, Keyimu et al. 2020b). Temperature is an important stressor on cambium activity during the growth season (Körner 1998). At a sufficient temperature, carbohydrates provide energy through photosynthetic activity which is required in the formation and enlargement of tracheid cells of conifers near the timber line (Deslauriers et al. 2008, Rossi et al. 2008). Our results showed that the radial growth of Faxon fir on Zhegu Mountain was significantly correlated with the maximum temperature in autumn (Fig. 4). The favorable climate in the final

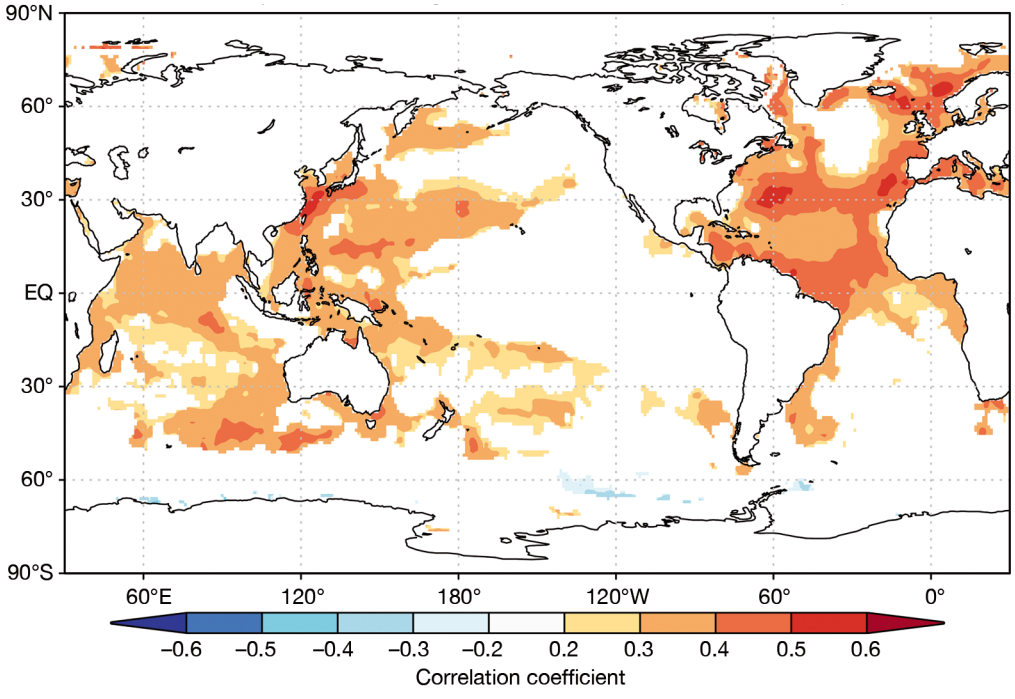

Fig. 10. Reconstructed temperature with the gridded sea-surface temperature (SST) data set of HadISST1 1° over the overlapping period from 1870–2016. The analyses were performed using the KNMI climate explorer (Royal Netherlands Meteorological Institute; http://climexp.knmi.nl)

Table 3. Information of volcanic eruptions considered in the present study. VEI: Volcanic Explosivity Index

	Event year	Volcano and region	Latitude	Longitude	VEI
1	1862	Makian, Indonesia	0.3° N	127.4° E	5
2	1883	Krakatau, Indonesia	6.1° S	105.4° E	6
3	1912	Novarupta (Katmai), Alaska, USA	58.3° N	155.2° W	6
4	1956	Bezymianny, Russia	56.0° N	160.6° E	5
5	1983	El Chichon, Mexico	17.4° N	93.2° W	5
6	1991	Pinatubo, Philippines	15.1° N	120.4° E	6

growth phase affects tree-ring latewood formation in this season (Duan et al. 2010, Franceschini et al. 2013). The higher temperature during the autumn continues stimulating the tracheid cells, thus increasing the number of cells and cell wall thickness, which, as a result, widen the tree-ring width. Previous studies near tree line sites in the Hengduan Mountains also suggested the regulating function of autumn temperatures on the growth of evergreen conifers at high elevations (Bräuning 2006, Li et al. 2015; Zhu et al. 2016). Our climate–tree growth response analysis demonstrated that winter temperature also positively influenced inter-annual radial growth of Faxon firs on Zhegu Mountain. The importance of non-growing season temperature on radial tree growth was evidenced by other studies which were conducted in the high altitudes of Tibet and the Hengduan Mountains (Bräuning 2001, Liang et al. 2006, 2008, Fan et al. 2009, Li et al. 2011). The influence of winter temperature on radial tree growth can be explained by several mechanisms. Winter temperature, especially maximum temperature, reduces the cold damage on conifer leaves, which minimizes the threat to leaf metabolic activity (Mayr et al. 2007). Therefore, temperate coniferous trees still be photosynthetically active and assimilate carbon during warmer winter days when they have unfrozen leaves (Tardif & Stevenson 2001). Additionally, the maximum winter temperature also reduces the cold damage to fine roots, indirectly contributing to tree growth in the following season, because the energy which could be spent on the recovery of damaged roots would likely be used on the activation of the cambium layer instead, which contributes to tree radial growth and carbon uptake.

The previous-year climate has a legacy effect on current-year tree growth (Fritts 1976, Wu et al. 2018). Our results demonstrated the strong legacy effect of the previous year's maximum temperature on the radial tree growth in the current year, because tree growth in the current year, especially in spring, usually involves the photosynthetic products stored in the parenchyma structure of the tree stem during the previous growing season (Fritts 1976). Our results are concordant with empirical reports from the Tibetan Plateau and its southeastern edge (Fan et al. 2009, Li et al. 2011, Keyimu et al. 2020b).

4.2. Comparisons of our reconstruction with other records

To assess the spatial representativeness of our reconstruction, we compared the series with 3 other records from surrounding regions (Fig. 8), including the annual mean temperature reconstruction in the western Sichuan Province of China (Li et al. 2015), the warm season (April–September) mean temperature reconstruction in the central Hengduan Mountains (Fan et al. 2009), and the annual mean minimum temperature reconstruction in the southeastern Tibetan Plateau (Keyimu et al. 2020b). All of these reconstructions, including ours, were normalized and smoothed with an 11 yr moving average (Fig. 8). The warm episodes of the 1860s, 1945–1955, and post-1995 on Zhegu Mountain in the present study are consistent with the warm periods of 1860–1865, 1930s–1960s, and post-1995 in western Sichuan reported by Li et al. (2015); with warm episodes of 1950s–1960s and 1995 in the central Hengduan Mountains reported by Fan et al. (2009); and warm periods of 1860s, 1940s–1965, and post-1990s in the southeastern Tibetan Plateau reported by Keyimu et al. (2020b). The cold periods of 1885–1995, 1905–1925, and 1970s–1990s were also in agreement with cold episodes of 1890s, 1910–1915, and 1975–1990s reported by Li et al. (2015); with cold periods of 1890s, 1910–1915, and 1980s–1990s in the study by Fan et al. (2009); and with 1910–1915, and 1975–1990s reported by Keyimu et al. (2020b). The spatial correlation field of the reconstructed TMX series with the regionally gridded maximum temperature dataset for the period 1954 2016 (Fig. 9) demonstrated that the reconstructed temperature series could represent the climate conditions for a large territory in the western Sichuan Plateau of China.

However, there were also evident discrepancies among the reconstructions. For instance, our reconstruction identified 1945–1955s as a warm period, whereas Li et al. (2015) identified the 1930s–1960s as

warm, and Fan et al. (2009) identified the 1950s–1960s as warm. The length of the cold period in our reconstruction was about 20 yr (1905–1925), whereas it was only about 10 yr (1905–1915) in the reconstruction by Li et al. (2015). Our series showed high temperatures during the 1900s, while the series of Li et al. (2015) and Keyimu et al. (2020b) demonstrated these as cold years. This might be due to differences in specific reconstruction time, tree species, and the different detrending approach adopted for tree-ring data (Thapa et al. 2015), as well as the potential modulation of local climate conditions.

We also compared the featured changes in temperature with investigations from more distant sites to find evidence supporting the spatial synchrony of climate variation. The temperature reconstruction series of Shao & Fan (1999) from the western Sichuan Plateau was partly close to our reconstruction. Their warm episodes of the 1900s, 1950s, and 1995 and the cold periods of 1885, 1910s, and 1990s were in agreement with our results. It is worth noting that the relatively longer period of cold in the 20th century occurred during 1905–1925. Such severe cold was evidenced by other tree-ring records (Shao & Fan 1999, Bräuning 2006, Gou et al. 2007, Zhang et al. 2014, Liang et al. 2016) as well as ice cores (Yao et al. 2006) from the Tibetan Plateau. There was a warm period (1950s–1965) as well, which was in accordance with a warm episode in the Himalayas (Cook et al. 2003, Lv & Zhang 2013) and the central (Liang et al. 2008, He et al. 2014) and northeastern (Gou et al. 2007) Tibetan Plateau. One of the featured cold episodes in the last century spanned 1965–1985. From 1965, the temperature began to decrease dramatically, especially during cold episodes in the intervals of 1970–1974 and 1977–1980. This decrease was also identified in the reconstruction series from nearby areas (Yadav et al. 2004, Li et al. 2015, Li & Li 2017), as well as in some other reconstructed temperature series from more distant locations (Briffa et al. 1998, Chen et al. 2010). Although the EPS of our chronology was below 0.85 before 1869 due to the reduced sample size (but larger than 5), the concordant cold and warm episodes with other reconstructions from surrounding regions implied the reliability of our reconstruction series.

4.3. Significant cycles in the reconstruction and natural forces

To investigate the spatial linkage of our aggregated autumn and winter TMX reconstruction series for Zhegu Mountain with climate systems on a global level, we correlated our reconstruction with global sea surface temperature (SST) reconstruction (HadISST1 1°) during the common time series of 1870–2016 using KNMI Climate Explorer (Fig. 10). We can observe the positive correlation between the reconstruction series with Western Pacific SST which indicates the relationships between reconstruction and the Asian–Pacific Oscillation (APO). The APO is induced by large-scale thermal differences between the land and sea (Duan & Wu 2005), affecting the climate of large parts of China. To further investigate the relationship, we correlated the reconstructed series with the APO index reported by Zhao et al. (2008); after smoothing with an 11 yr moving average for the common interval of 1861–1980, the significant correlation ($R = 0.47$, $p < 0.001$) confirmed the linkage between regional TMX reconstruction and the western Pacific Ocean activity. Fig. 10 also demonstrates the positive correlation of TMX reconstruction with North Atlantic SST, which implied the impact of the Atlantic Multidecadal Oscillation (AMO) on the regional climate system. Kerr (2000) reported that the AMO potentially affects large-scale atmospheric circulation over the Eurasian continent. We used the annual AMO indices reconstructed by Mann et al. (2009) from the KNMI climate explorer (http://climexp.knmi.nl/getindices.cgi?WMO=RapidData/amo_mann&STATION) and compared it to our reconstruction series for the common period of 1856–2006. A significant and positive correlation ($R = 0.46$, $p < 0.001$) confirmed the connection between the temperature fluctuation on Zhegu Mountain and activity in the North Atlantic Ocean.

Another natural force which impacts the climate system is solar activity. There is a close relationship between solar activity and the Earth's surface temperature (Duan & Zhang 2014). Sun spots are among the most basic and obvious phenomena of solar activity (Cai et al. 2014). Decadal and multi-decadal variations in reconstructions are usually associated with the sunspot number (Panthi et al. 2017, Chen et al. 2019a). To further investigate the influence of solar activity on the alteration of regional warm and cold conditions on Zhegu Mountain, we downloaded the annual sun spot number (http://climexp.knmi.nl/getindices.cgi?WMO=SIDCData/sunspots&STATION=sunspots) to conduct a correlation analysis with our reconstruction series. The mid- and low-frequency variations of the 2 indices after 11 and 31 yr smoothing showed a significant correlation with each other ($R = 0.41$, $p < 0.001$; and $R = 0.54$, $p < 0.001$), respectively. This convincingly supported the in-

fluence of solar activity on the alterations of warm and cold conditions in the Zhegu Mountain area of western Sichuan. Our result indicating a connection between historical temperature and solar activity is in agreement with an investigation by Zhu et al. (2016) conducted in the northwestern Sichuan Plateau.

Volcanic activity is one of the biggest environmental impacts on Earth's climate. Tree-ring-based regional temperature reconstructions have demonstrated matches between regional cold episodes, temperature decrease, and dates of some volcanic activities around the globe (Briffa et al. 1998, Salzer & Hughes 2007, Mann et al. 2012, Sigl et al. 2015, Chen et al. 2019b). The length of such cold periods is impacted by the frequency and magnitude of large volcanic eruptions. We selected 6 larger volcanic eruptions in history (shown in Fig. 7b) and conducted SE analysis; the results confirmed the cooling effect of volcanic eruptions (Fig. 11). We observed 3 major cold periods in the study area based on our temperature reconstruction. The first one is 1883–1886, and this may be linked to the Krakatau volcanic eruption in western Java, Indonesia. The second coldest episode lasted from 1902 until the 1920s. This period saw a series of volcanic eruptions, the first of which was the Santa Maria eruption in Guatemala in 1902. The Santa Maria eruption was so large that its column was nearly 30 km high, and reached the stratosphere

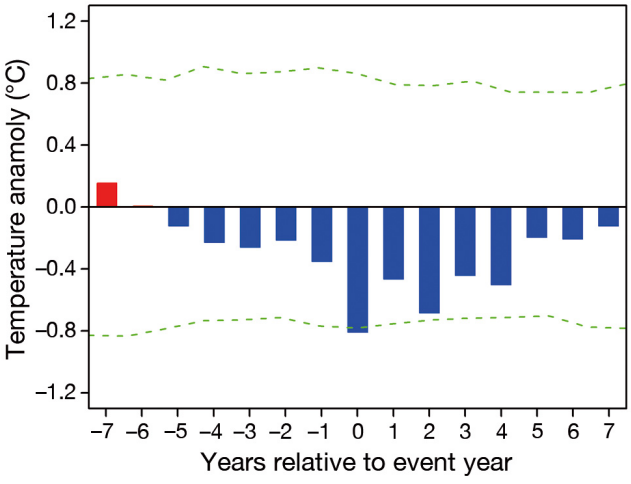

Fig. 11. Results of the superposed epoch analysis testing the impact of explosive volcanism on the reconstructed maximum temperature of aggregated seasons of autumn and winter on Zhegu Mountain during the period 1856–2016. Upper and lower horizontal dashed lines indicate the 95% significance level. Red and blue bars represent the positive and negative temperature anomalies, respectively

(Williams & Self 1983). The second volcanic eruption was the Ksudach Caldera Complex in 1907, located in the southern part of the Kamchatka Peninsula of Russia (Macaas & Sheridan 1995). The third one was the Novarupta volcanic eruption in Southern Alaska, USA, in June 1912, which was the most powerful eruption of the 20th century. It was reported that the Novarupta eruption weakened the Indian summer monsoon during the following years (Rafferty 2012). The prevailing cold from 1902–1920s is also confirmed by other tree-ring records and ice-core investigations in the Tibetan Plateau (Bräuning 2006, Yao et al. 2006). The third cold episode occurred during the 1990s and was linked to the Pinatubu volcanic eruption in the Philippines, the second largest eruption in the last century. These eruptions influenced the atmospheric circulation patterns (Free & Lanzante 2009), causing dramatic temperature decreases and declines in radial tree growth.

5. CONCLUSION

We built a chronology using tree-ring width data of Faxon fir near the timberline of Zhegu Mountain in the Miyaluo Scenic Area, western Sichuan Plateau. Climate–growth response analysis showed that fir trees at the timberline were temperature sensitive; in particular, the relationship between interannual radial tree growth and maximum temperature was comparatively stronger. A linear model between chronology and climate accounted for 43.2% of the aggregated maximum temperature of autumn and winter. Based on this model, we reconstructed 161 yr of aggregated autumn and winter maximum temperature for the study area. The reconstruction results were in agreement with other records of tree-ring-based temperature reconstructions from nearby regions, confirming the reliability of our investigation. The relationship between the reconstruction series and SST indicated a linkage of regional climate with global-scale sea–atmospheric circulations. We also concluded that the solar activity and volcanic eruptions exerted a strong influence on the temperature fluctuation in the investigated area. Our reconstruction series helps to fill the gap in the spatial coverage of proxy-based climate records in the high-elevation areas of the western Sichuan Plateau. However, the tree-ring network should be expanded (sampling site and chronology length) in the future to further understand the historical climatic condition and its variability in this region.

Acknowledgements. This work was funded by the National Key Research Development Program of China (2016YFC 0502105), the Second Tibetan Plateau Scientific Expedition and Research (STEP) program (2019QZKK0502), and the National Natural Science Foundation of China (NSFC, 31770533). The monthly climate data used in this study were obtained from the National Meteorological Information Center (NMIC) of China. We thank Dr. Xian Cheng from Southwest University of China for his technical assistance on graphing. We are very grateful to the anonymous reviewers for their valuable comments on this article.

LITERATURE CITED

Allen KJ, Anchukaitis KJ, Grose MG, Lee Gand others (2019) Tree-ring reconstructions of cool season temperature for far southeastern Australia, 1731–2007. Clim Dyn 53:569–583

Björklund J, von Arx G, Nievergelt D, Wilson R and others (2019) Scientific merits and analytical challenges of tree-ring densitometry. Rev Geophys 57:1224–1264

Bräuning A (2001) Combined view of various tree ring parameters from different habitats in Tibet for the reconstruction of seasonal aspects of Asian Monsoon variability. Palaeobotanist 50:1–12

Bräuning A (2006) Tree-ring evidence of 'little ice age' glacier advances in southern Tibet. Holocene 16:369–380

Briffa KR, Jones PD, Schweingruber FH, Karlén W, Shiyatov SG (1996) Tree-ring variables as proxy-climate indicators: problems with low-frequency signals. In: Jones PD, Bradley RS, Jouzel J (eds) Climatic variations and forcing mechanisms of the last 2000 years. NATO Adv Stud Inst Ser I Global Environ Change, Vol 41. Springer, Berlin, p 9–41

Briffa KR, Jones PD, Schweingruber FH, Osborn TJ (1998) Influence of volcanic eruptions on northern hemisphere summer temperature over the past 600 years. Nature 393:450–455

Cai QF, Liu Y, Lei Y, Bao G, Sun B (2014) Reconstruction of the March–August PDSI since 1703 AD based on tree rings of Chinese pine (*Pinus tabulaeformis* Carr.) in the Lingkong Mountain, southeast Chinese loess Plateau. Clim Past 10:509–521

Chen F, Yuan Y, Wei W, Yu S and others (2010) Reconstruction of annual precipitation in Shandan, since 1783 A.D. Geogr Geo-Inform Sci 26:82–86 (in Chinese with English abstract)

Chen F, Shang HM, Panyushkina I, Meko D and others (2019a) 500-year tree-ring reconstruction of Salween River streamflow related to the history of water supply in Southeast Asia. Clim Dyn 53:6595–6607

Chen F, Yuan YJ, Yu SL, Chen FH (2019b) A 391-year summer temperature reconstruction of the Tien Shan, reveals far-reaching summer temperature signals over the mid-latitude Eurasian continent. J Geophys Res Atmos 124: 11850–11862

Cook ER, Briffa KR, Meko DM, Graybill DA, Funkhouser G (1995) The 'segment length curse' in long tree-ring chronology development for palaeoclimatic studies. Holocene 5:229–237

Cook ER, Krusic PJ, Jones PD (2003) Dendroclimatic signals in long tree-ring chronologies from the Himalayas of Nepal. Int J Climatol 23:707–732

D'Arrigo R, Baker P, Palmer J, Anchukaitis K, Cook G (2008) Experimental reconstruction of monsoon drought variability for Australasia using tree rings and corals. Geophys Res Lett 35:L12709

Deslauriers A, Rossi S, Anfodillo T, Saracino A (2008) Cambial phenology, wood formation and temperature thresholds in two contrasting years at high altitude in southern Italy. Tree Physiol 28:863–871

Duan AM, Wu GX (2005) Role of the Tibetan Plateau thermal forcing in the summer climate patterns over subtropical Asia. Clim Dyn 24:793–807

Duan J, Zhang QB (2014) A 449 year warm season temperature reconstruction in the southeastern Tibetan Plateau and its relation to solar activity. J Geophys Res Atmos 119:11578–11592

Duan JP, Wang L, Lun L, Chen KL (2010) Temperature variability since A.D. 1837 inferred from tree-ring maximum density of *Abies fabri* on Gongga Mountain, China. Sci Bull (Beijing) 55:3015–3022

Esper J, Cook ER, Schweingruber FH (2002) Low-frequency signals in long tree-ring chronologies for reconstructing past temperature variability. Science 295:2250–2253

Esper J, Büntgen U, Timonen M, Frank DC (2012) Variability and extremes of northern Scandinavian summer temperatures over the past two millennia. Global Planet Change 88-89:1–9

Fan ZX, Bräuning A, Yang B, Cao KF (2009) Tree ring density-based summer temperature reconstruction for the central Hengduan Mountains in southern China. Global Planet Change 65:1–11

Franceschini T, Bontemps JD, Perez V, Leban JM (2013) Divergence in latewood density response of Norway spruce to temperature is not resolved by enlarged sets of climatic predictors and their non-linearities. Agric For Meteorol 180:132–141

Free M, Lanzante J (2009) Effect of volcanic eruptions on the vertical temperature profile in radiosonde data and climate models. J Clim 22:2925–2939

Fritts HC (1976) Tree rings and climate. Academic Press, London

Gou X, Chen FH, Jacoby G, Cook E, Yang MX, Peng JF, Zhang Y (2007) Rapid tree growth with respect to the last 400 years in response to climate warming, northeastern Tibetan Plateau. Int J Climatol 27:1497–1503

Gou XH, Gao LL, Deng Y, Chen FH, Yang MX, Still C (2015) An 850-year tree-ring-based reconstruction of drought history in the western Qilian Mountains of northwestern China. Int J Climatol 35:3308–3319

He M, Yang B, Datsenko NM (2014) A six hundred-year annual minimum temperature history for the central Tibetan Plateau derived from tree-ring width series. Clim Dyn 43:641–655

Holmes RL (1983) Computer-assisted quality control in tree-ring dating and measurement. Tree-Ring Bull 43: 69–75

Huang R, Zhu H, Liang E, Liu B and others (2019) A tree ring-based winter temperature reconstruction for the southeastern Tibetan Plateau since 1340 CE. Clim Dyn 53:3221–3233

IPCC (2013) Climate change 2013: the physical science basis. Contribution of Working Group I to the Fifth Assessment Report of the Intergovernmental Panel on Climate Change. Cambridge University Press, Cambridge

Jiménez-Moreno G, Fauquette S, Suc JP (2010) Miocene to Pliocene vegetation reconstruction and climate estimates in the Iberian Peninsula from pollen data. Rev Palaeobot Palynol 162:403–415

Kerr RA (2000) A North Atlantic climate pacemaker for the centuries. Science 288:1984–1985

Keyimu M, Wei JS, Zhang YX, Zhang S, Li ZS, Ma KM, Fu BJ (2020a) Climate signal shift under the influence of prevailing climate warming — evidence from *Quercus liaotungensis* on Dongling Mountain, Beijing, China. Dendrochronologia 60:125683

Keyimu M, Li ZS, Zhang GS, Fan ZX, Wang XC, Fu BJ (2020b) Tree ring based minimum temperature reconstruction in the central Hengduan Mountains, China. Theor Appl Climol 141:359–370

Körner C (1998) A re-assessment of high elevation treeline positions and their explanation. Oecologia 115:445–459

Li T, Li JB (2017) A 564-year annual minimum temperature reconstruction for the east central Tibetan Plateau from tree rings. Global Planet Change 157:165–173

Li ZS, Liu GH, Zhang QB, Hu CJ, Luo SZ, Liu XL, He F (2010) Tree ring reconstruction of summer temperature variations over the past 159 years in Wolong National Natural Reserve, western Sichuan, China. Acta Phytoecol Sin 34:628–641 (in Chinese with English abstract)

Li Z, Shi CM, Liu Y, Zhang J, Zhang Q, Ma K (2011) Summer mean temperature variation from 1710–2005 inferred from tree-ring data of the Baimang Snow Mountains, northwestern Yunnan, China. Clim Res 47:207–218

Li ZS, Liu GH, Gong L, Wang M, Wang XC (2015) Tree ring-based temperature reconstruction over the past 186 years for the Miyaluo natural reserve, western Sichuan province of China. Theor Appl Climatol 120:495–506

Liang EY, Shao XM, Eckstein D, Huang L, Liu X (2006) Topography-and species-dependent growth responses of *Sabina przewalskii* and *Picea crassifolia* to climate on the northeast Tibetan Plateau. For Ecol Manag 236:268–277

Liang E, Shao X, Qin N (2008) Tree-ring based summer temperature reconstruction for the source region of the Yangtze River on the Tibetan Plateau. Global Planet Change 61:313–320

Liang HX, Lv LX, Wahab M (2016) A 382-year reconstruction of August mean minimum temperature from tree-ring maximum latewood density on the southeastern Tibetan Plateau, China. Dendrochronologia 37:1–8

Lv LX, Zhang QB (2013) Tree-ring based summer minimum temperature reconstruction for the southern edge of the Qinghai-Tibetan Plateau, China. Clim Res 56:91–101

Macáas JL, Sheridan MF (1995) Products of the 1907 eruption of Shtyubel′ Volcano, Ksudach Caldera, Kamchatka, Russia. Bull Geol Soc Am 107:969–986

Mann ME, Zhang ZH, Rutherford S, Bradley RS and others (2009) Global signatures and dynamical origins of the little ice age and medieval climate anomaly. Science 326: 1256–1260

Mann ME, Fuentes JD, Rutherford S (2012) Underestimation of volcanic cooling in tree-ring-based reconstructions of hemispheric temperatures. Nat Geosci 5:202–205

Mayr S, Cochard H, Ameglio T, Kikuta SB (2007) Embolism formation during freezing in the wood of *Picea abies*. Plant Physiol 143:60–67

Mitchell TD, Jones PD (2005) An improved method of constructing a database of monthly climate observations and associated high-resolution grids. Int J Climatol 25: 693–712

Pang X, Ning W, Qing L, Bao W (2009) The relation among soil microorganism, enzyme activity and soil nutrients under subalpine coniferous forest in western Sichuan. Acta Ecol Sin 29:286–292 (in Chinese with English abstract)

Panthi S, Bräuning A, Zhou ZK, Fan ZX (2017) Tree rings reveal recent intensified spring drought in the central Himalaya, Nepal. Global Planet Change 157:26–34

Pilcher JR, Baillie MGL, Schmidt B, Becker B (1984) A 7,272-year tree-ring chronology for western Europe. Nature 312:150–152

Proctor CJ, Baker A, Barnes WL, Gilmour MA (2000) A thousand year speleothem proxy record of north Atlantic climate from Scotland. Clim Dyn 16:815–820

R Core Team (2019) R: a language and environment for statistical computing. R Foundation for Statistical Computing, Vienna

Rafferty J (2012) Novarupta volcano, Alaska, United States. Earth and Life Sciences at Encyclopaedia Britannica. www.britannica.com/place/Novarupta

Rossi S, Deslauriers A, Gricar J, Seo JW and others (2008) Critical temperatures for xylogenesis in conifers of cold climates. Glob Ecol Biogeogr 17:696–707

Salzer MW, Hughes MK (2007) Bristlecone pine tree rings and volcanic eruptions over the last 5000 yr. Quat Res 67: 57–68

Schweingruber FH (1996) Tree rings and environment: dendroecology, Haupt, Bern

Shao XM, Fan JM (1999) Past climate on west Sichuan Plateau as reconstructed from ring-widths of dragon spruce. Quat Sci 1:81–89 (in Chinese with English abstract)

Sigl M, Winstrup M, McConnell JR, Welten KC and others (2015) Timing and climate forcing of volcanic eruptions for the past 2,500 years. Nature 523:543–549

Song HM, Liu Y, Ni WM, Cai QF, Sun JY, Ge WB, Xiao WY (2007) Winter mean lowest temperature derived from tree-ring within Jiuzhaigou region, China since 1750 A. D. Quat Sci 27:486–491 (in Chinese with English abstract)

Steiger NJ, Steig EJ, Dee SG, Roe GH, Hakim GJ (2017) Climate reconstruction using data assimilation of water isotope ratios from ice cores. J Geophys Res Atmos 122: 1545–1568

Stokes MA, Smiley TL (1996) An introduction to tree-ring dating. Arizona University Press, Tucson, AZ

Tardif J, Stevenson D (2001) Radial growth-climate association of *Thuja occidentalis* L. at the northwestern limit of its distribution, Manitoba, Canada. Dendrochronologia 19:179–187

Thapa UK, Shah SK, Gaire NP, Bhuju DR (2015) Spring temperatures in the far-western Nepal Himalaya since ad 1640 reconstructed from *Picea smithiana* tree-ring widths. Clim Dyn 45:2069–2081

Vaks A, Bar-Matthews M, Ayalon A, Schilman B and others (2003) Paleoclimate reconstruction based on the timing of speleothem growth and oxygen and carbon isotope composition in a cave located in the rain shadow in Israel. Quat Res 59:182–193

Williams SN, Self S (1983) The October 1902 Plinian eruption of Santa Maria volcano, Guatemala. J Volcanol Geotherm Res 16:33–56

Wilson RJS, Luckman BH (2002) Tree-ring reconstruction of maximum and minimum temperatures and the diurnal temperature range in British Columbia, Canada. Dendrochronologia 20:257–268

Wu X, Liu H, Li X, Ciais P and others (2018) Differentiating drought legacy effects on vegetation growth over the temperate Northern Hemisphere. Glob Change Biol 24: 504–516

Yadav RR, Park WK, Singh J, Dubey B (2004) Do the western Himalayas defy global warming? Geophys Res Lett 31: L17201

Yang B, Qin C, Wang J, He M, Melvin TM, Osborn TJ, Briffa KR (2014) A 3,500-year tree-ring record of annual precipitation on the northeastern Tibetan Plateau. Proc Natl Acad Sci USA 111:2903–2908

Yao TD, Qin DH, Xu BQ, Yang MX and others (2006) Temperature change over the past millennium recorded in ice cores from the Tibetan Plateau. Adv Clim Chang Res 2:99–103 (in Chinese with English abstract)

Yin H, Liu H, Linderholm HW, Sun Y (2015) Tree ring density-based warm-season temperature reconstruction since A.D. 1610 in the eastern Tibetan Plateau. Palaeogeogr Palaeoclimatol Palaeoecol 426:112–120

Zech J, Zech R, Kubik PW, Veit H (2009) Glacier and climate reconstruction at Tres Lagunas, NW Argentina, based on ^{10}Be surface exposure dating and lake sediment analyses. Palaeogeogr Palaeoclimatol Palaeoecol 284:180–190

Zhang QB, Cheng GD, Yao TD, Kang XC, Huang JG (2003) A 2326-year tree-ring record of climate variability on the northeastern Qinghai-Tibetan Plateau. Geophys Res Lett 30:1739–1742

Zhang QY (2006) Ecological characteristics of timberline tree populations in eastern Qinghai-Tibetan Plateau. PhD dissertation, Chinese Academy of Sciences, Beijing (in Chinese with English abstract)

Zhang Y, Shao XM, Yin ZY, Wang Y (2014) Millennial minimum temperature variations in the Qilian Mountains, China: evidence from tree rings. Clim Past 10:1763–1778

Zhao P, Chen JM, Xiao D, Nan SL, Zou Y, Zhou BT (2008) Summer Asian-Pacific oscillation and its relationship with atmospheric circulation and monsoon rainfall. Acta Meteorol Sin 22:455–471

Zhu L, Zhang Y, Li ZS, Guo B, Wang X (2016) A 368-year maximum temperature reconstruction based on tree-ring data in the northwestern Sichuan Plateau (NWSP), China. Clim Past 12:1485–1498

Editorial responsibility: Guoyu Ren, Beijing, PR China

Submitted: March 17, 2020; Accepted: May 29, 2020
Proofs received from author(s): June 26, 2020